Climatic Change (2013) 116:705–722
DOI 10.1007/s10584-012-0504-7

Changes in extreme daily rainfall for São Paulo, Brazil

Maria A. F. Silva Dias · Juliana Dias · Leila M. V. Carvalho · Edmilson D. Freitas · Pedro L. Silva Dias

Received: 2 November 2011 / Accepted: 20 May 2012 / Published online: 7 June 2012

Abstract Significant positive trends are found in the evolution of daily rainfall extremes in the city of São Paulo (Brazil) from 1933 to 2010. Climatic indices including ENSO, PDO, NAO and the sea surface temperature at the coast near São Paulo explain 85 % of the increasing frequency of extremes during the dry season. During the wet season the climatic indices and the local sea surface temperature explain a smaller fraction of the total variance when compared to the dry season indicating that other factors such as the growth of the urban heat island and the role of air pollution in cloud microphysics need to be taken into account to explain the observed trends over the almost eight decades.

1 Introduction

Global and regional climate have evolved during the last century due to natural and anthropogenic influences with associated changes in rainfall amounts and rainfall

Electronic supplementary material The online version of this article (doi:10.1007/s10584-012-0504-7) contains supplementary material, which is available to authorized users.

M. A. F. Silva Dias (✉) · E. D. Freitas
Departamento de Ciências Atmosféricas, Universidade de São Paulo, São Paulo, Brazil
e-mail: mafdsdia@model.iag.usp.br

E. D. Freitas
efreitas@model.iag.usp.br

J. Dias
Earth System Research Laboratory, NOAA, Boulder, CO, USA
e-mail: juliana.dias@noaa.gov

L. M. V. Carvalho
University of California at Santa Barbara, Santa Barbara, CA, USA
e-mail: leila@eri.ucsb.edu

P. L. Silva Dias
Departamento de Ciências Atmosféricas, Universidade de São Paulo, São Paulo, Brazil
email: pldsdias@lncc.br

P. L. Silva Dias
Laboratório Nacional de Computação Científica, Petrópolis, Brazil

patterns (IPCC 2007). Haylock et al. (2006), among others, discuss the rainfall change in South America from 1960 to 2000 relating the observed changes to sea surface temperature (SST) anomalies like the ENSO cycles. Marengo et al. (2001) indicate that the duration, onset and withdrawal of the rainy season in Brazil show considerable interannual variability and are also linked to Atlantic and Pacific SST patterns. Berbery et al. (2006) indicate that in the southeastern region of South America there has been a shift to the west of the maximum values of yearly rainfall totals over the last four decades of the 20th Century.

The effect of large urban areas on rainfall is also a subject that has been extensively studied. Perhaps the more comprehensive research was the one performed in the St Louis area by the METROMEX (Chagnon 1979; Changnon et al. 1991) where rainfall was seen to increase between 5 and 25 % downwind from the city area. More recently, Shepherd et al. (2002) using the TRMM satellite precipitation radar data studied many cities in the USA and confirmed the same tendency of rainfall augmentation in the urban area and downwind from it, not only in accumulated values but also an increase in the maximum rainfall rate.

Several authors have attempted to separate the effects of large scale climate variability from regional and local effects in climate due to land use or land cover changes. In the case of temperature, Kalnay and Cai (2003) estimate the impact of urbanization by comparing trends measured in cities with those reconstructed from a reanalysis (Kalnay et al. 1996) that is virtually insensitive to surface data. They suggest that half the reduction in daily temperature range over cities in the United States and up to 1.4 °C of the increase in temperature—over 40 years—are due to urbanization. The same approach in the case of rainfall would be complicated by the fact that rainfall is a discrete variable not so well reproduced as temperature by the reanalysis (Janowiak et al. 1998), mainly in regions of complex topography where several non-linear interactions may lead to rainfall increase or decrease. Rana et al. (2011) have used climatic indices to explain the changes in rainfall over large cities in India, where rainfall has shown different trends over the seasons. They conclude that most of the observed changes in daily rainfall over decades can be explained by large scale climate variability.

This paper looks into a time series of daily rainfall for a climatological station in the Metropolitan Area of São Paulo, MASP, in Brazil (Fig. 1). The MASP went from less than 2 million inhabitants in 1940 to almost 20 million by 2010 (Fig. 2a), a 10-fold increase in population that places the city among the 5 largest urban conglomerates in the world. According to the state of São Paulo Official site (http://www.emplasa.sp.gov.br) the urban area of the MASP shown in Fig. 2a, increased from 200 km^2 in 1930 to 2,407 km^2 in 2002, a factor of 12 in seven decades. The spatial evolution of the urban area has been reconstructed by an historical survey by Villaça (1978) for the 1881 to 1972 period; for 1982 to 1995 the area may be found in CESAD (http://www.cesadweb.fau.usp.br/index.php) and for 2002, the LANDSAT-5 TM satellite mosaic using channels 3, 4 and 5 has been used. The resulting area evolution may be seen in Fig. 2b. Before the 1960s, the several cities and small towns that today form the metropolitan area were scattered and surrounded by rural environment and did not constitute a contiguous urban area. The urban area gradually filled the rural gaps after the early 1960s (Fig. 2b).

Theoretical and modeling work have indicated that the increased sensible heat flux, heat sources and roughness of the urban areas are mechanisms for the formation of the urban heat island and the bifurcation of the flow upwind of the city area, which are important causes of the rainfall increase in and around large urban areas (e.g. Bornstein and Lin 2000; Carrió et al. 2010). Pollution effects may also play a significant role in controlling precipitation in

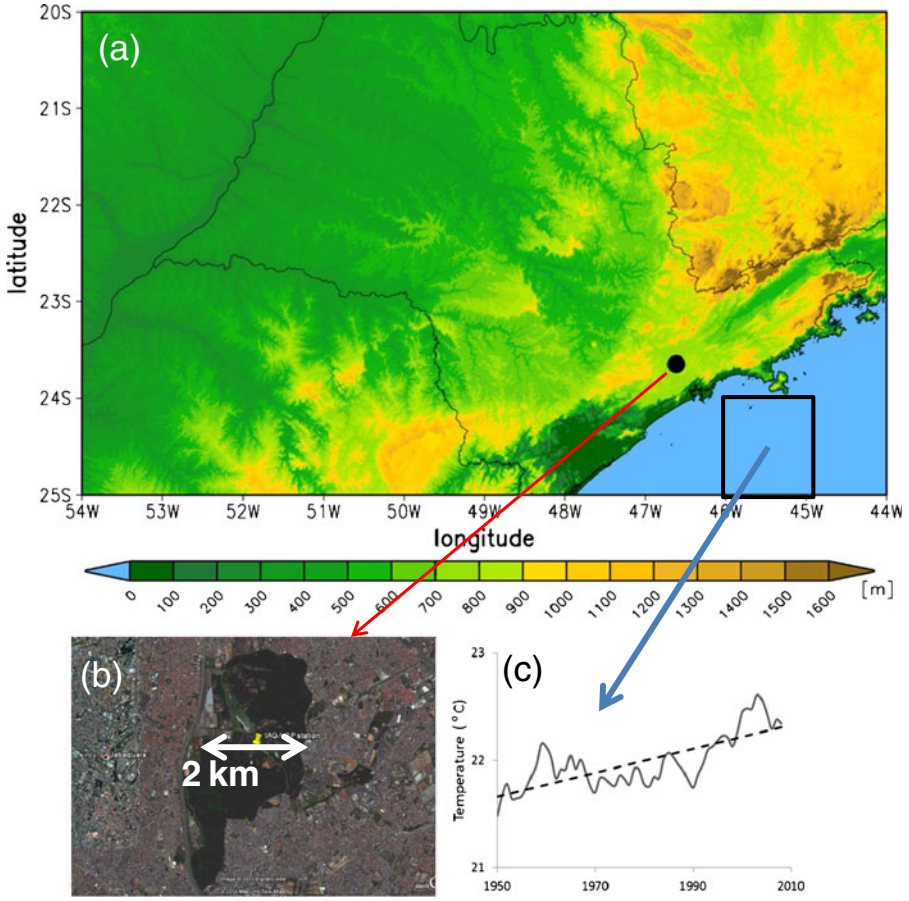

Fig. 1 **a** Topography of the region, *black circle* indicates the location of the IAG//USP station; *square* indicates the area used for averaging the SST index; **b** Google Earth view of the Parque do Estado with the *yellow pin* indicating the location of the IAG/USP station. *Dark areas* indicate vegetation. Around the park, the urban area. **c** Sea surface temperature (SST) evolution for the square indicated in Fig. 1a (from the NCEP reanalysis—Kalnay et al. 1996) and a linear fit

large urban areas primarily through the radiation balance with a cooling effect at the surface due to scattering of solar radiation by aerosols. This effect reduces the sensible heat flux at the surface and thus has a potentially negative impact on precipitation. However, Carrió and Cotton (2011) show a reversed effect in the Houston area (Texas, USA) where the aerosols act as cloud condensation nuclei (CCN), augmenting the maximum rainfall rate of the storms through cloud microphysical interactions except in the case of very high aerosol concentrations which lead to precipitation reduction in the numerical simulation.

The MASP is included in a region in Southern Brazil where Liebmann et al. (2001) indicate an increase in rainfall beginning in the 1950s. Penalba and Robledo (2010) showed that larger increases in rainfall in the La Plata Basin, in southeastern South America in the last 50 years, have occurred in the summer, spring and fall, especially for extreme events of daily rainfall. The MASP is located in the northeast border of the La Plata Basin.

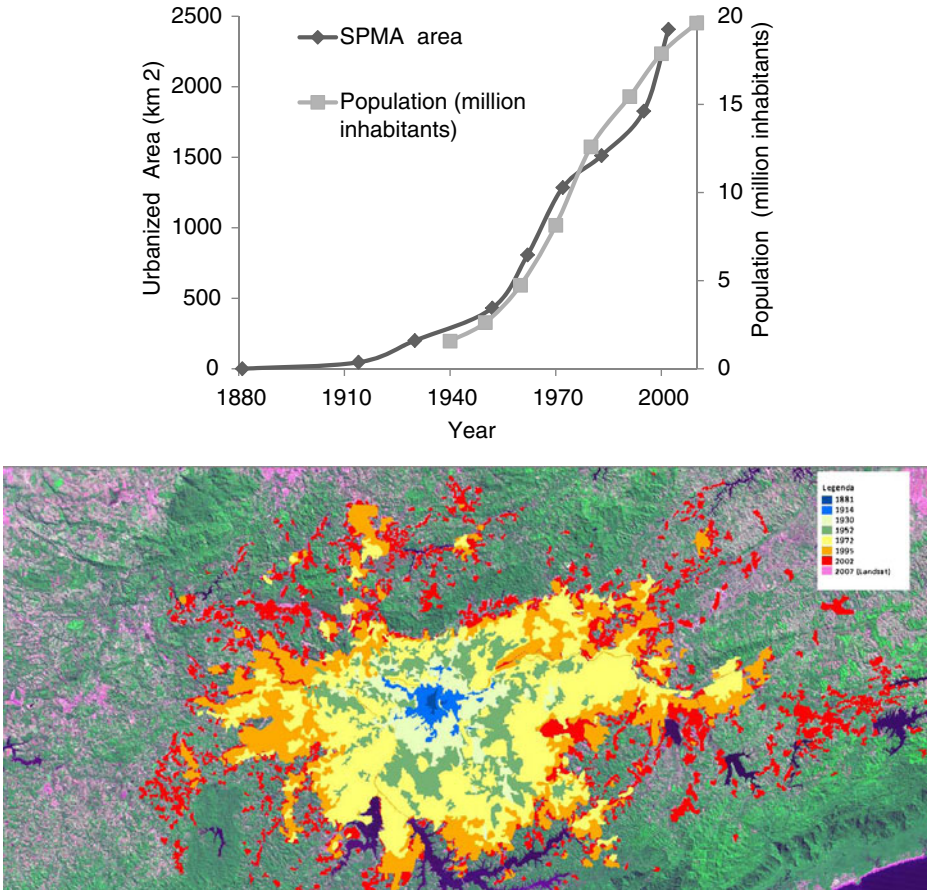

Fig. 2 **a** Number of inhabitants and area of the São Paulo Metropolitan area. From http://www.ibge.gov.br); **b** Evolution of Sao Paulo Metropolitan Area (Villaça 1978, CESAD, 1982 and 1995, and LANDSAT—5 TM, for 2002). The background is filled with a mosaic of LANDSAT satellite pictures (Ch 3, 4 and 5) for 2007

Another feature, peculiar to the MASP, is the proximity to the Atlantic Ocean coast line located 45 km southeast of the station used in the present work (see Fig. 1a). The sea-breeze coupled to the valley to mountain circulation penetrates towards the MASP plateau from the southeast (Silva Dias et al. 1995; Freitas et al. 2007) and may interact with the urban heat island, frequently triggering convective storms. Freitas et al. (2009) identified significant sensitivity of the numerically modeled rainfall over MASP on the sea surface temperature close to the coast: higher values of SST result in a weaker but moister circulation leading to enhanced rainfall. Lower values of coastal SST lead to stronger and drier circulation, and comparatively less rainfall. The coastal SST has been increasing in the last decades as may be seen in Fig. 1c. The presence of the urban area is also a factor that induces rainfall increase in the simulations.

With this background knowledge it is expected that as the urban area of the MASP increased through the last several decades, as well as the air pollution concentration, a corresponding change in rainfall should result. Attribution of causes of the observed changes

is, however, a complex task due to the evolving regional climate that has been seen to show positive rainfall trends in the region.

The focus in this paper is in the extreme daily rainfall events and how their frequency changes in the MASP from 1933 to 2010. Section 2 describes the data used in the study. The trends in the frequency of daily rainfall extremes are presented in Section 3. Possible explanations of the observed changes using climate variability, measured by large scale climate indices, are explored in Section 4 while Section 5 summarizes the main results.

2 Data

The rainfall data from 1933 to 2010 were obtained from the climatological station located in the center of a state park (Parque do Estado das Fontes do Ipiranga) at latitude 23°39′S, longitude 46°37′W and altitude of 799 m above sea level. The station is operated by the Institute of Astronomy, Geophysics and Atmospheric Sciences of the University of São Paulo (IAG/USP). The park was originally in a rural environment where an Astronomy Observatory was installed in 1933. Today the city surrounds the park in all directions as may be seen in Fig. 1b. However streets and avenues are at least 1 km away from the station. Terrain rises to about 950 m towards the coast and sharply drops to sea level 15 km southeast from the station. To the north-northwest at about 20 km from the IAG/USP station there is another mountain range (Serra da Cantareira), with altitude of the order of 1100 m so that most of the MASP and the IAG/USP station are located in a wide plateau. The distance of the station to the Atlantic Ocean coastline is 45 km.

There are no missing data in the daily rainfall series. The station has had a human observer since the beginning of operations in 1933 for a direct reading of the raingage and has a paper registry, the pluviograph, run by a mechanical clock. Sugahara et al. (2011) examined the daily rainfall series of this particular station and conclude that there is no inhomogeneity. Hourly rainfall data is also available as well as rainfall duration in minutes within the hour. Although there are other meteorological stations in the city area, none has such a complete record and the length of the IAG/USP station. The location is also particularly interesting when considering that it is surrounded by a park, close to the coast line and to the edge of the plateau where the city is located. This makes this station very special and justifies its use for the purpose of the present work.

Time series for climate indices have been obtained from http://www.esrl.noaa.gov/. The indices used are:

- PDO—Pacific Decadal Oscillation Index (Hurrell 1995; Zhang et al. 1997; Mantua et al. 1997)
- NAO—North Atlantic Oscillation (Chen and van den Dool 2003)
- AMC—Atlantic Meridional Circulation Index (Chiang and Vimont 2004)
- ENSO—Multivariate ENSO Index (Wolter and Timlin 1993)

Other climate indices used are:

- LISAM—The Large-scale Index for South America Monsoon obtained from Silva and Carvalho (2007). The original LISAM index has been normalized by removing the long term average and dividing by the standard deviation.

– SST—The sea surface temperature –, close to the coast line has been obtained from the NCEP reanalysis (Kalnay et al. 1996) and averaged over the area delimited by 24° S, 25° S and 45° W, 46° W and shown in Fig. 1c.

The annual average of each of the above climatic indices has been obtained and a five year running average performed.

3 Results

The average annual cycle of rainfall and its standard deviation for the 1933–2010 period at the IAG/USP station are shown in Fig. 3a. The wet season is from October through March.

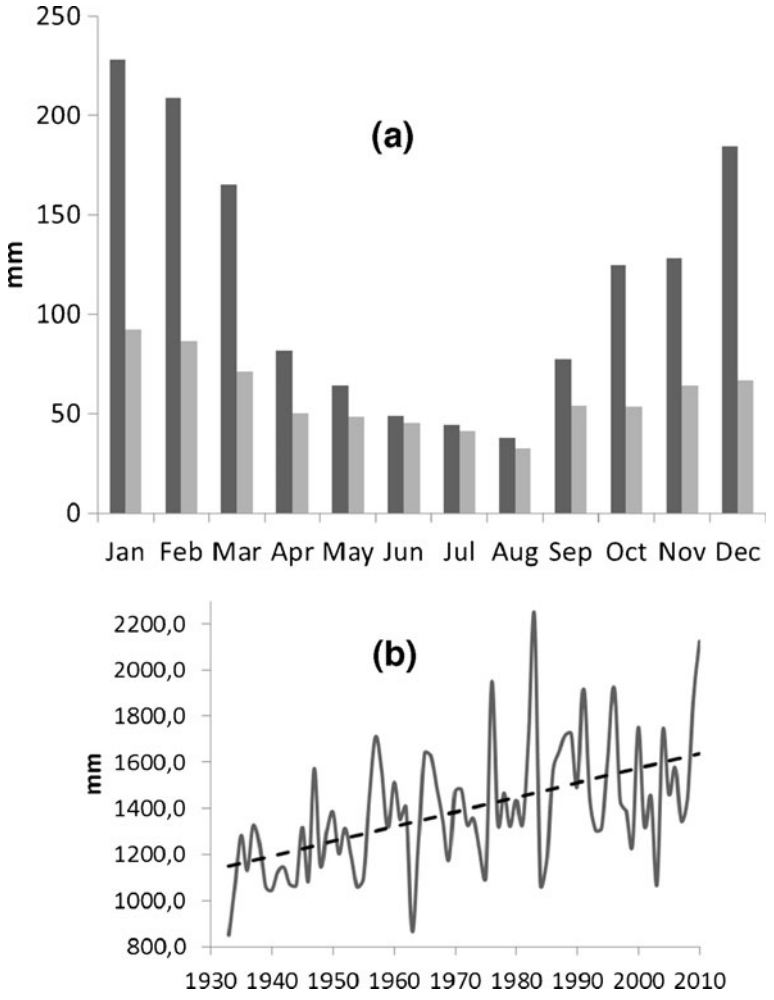

Fig. 3 **a** Average annual rainfall at IAG/USP station in *black* and standard deviation in *grey*, for the whole period from 1933 to 2010. **b** *Solid line* is the rainfall yearly total; *dashed line* represents a linear fit with r^2= 0.27. The Mann-Kendall test rejects the hypothesis of no trend at the level of 95 % with p<0.01. Slope= 5.518 mm/year

During the dry season, corresponding to the Southern Hemisphere winter, variability is quite high with standard deviations of about the same magnitude as the longtime average. Rainfall in the dry season is primarily due to frontal activity (Satyamurty et al. 1998). Figure 3b shows the evolution of the annual rainfall total for the same period. The increase in annual total rainfall has been noted for some time (e.g. Pereira Filho et al. 2007; Dufek and Ambrizzi 2008). From a linear fit the increase in yearly rainfall accumulation is 425 mm in 77 years or 5.5 mm/year. The linear trend explains 27 % of the total variance of the series.

The probability density function (PDF) for the daily rainfall has changed somewhat from the beginning of the series to the end. Using the first and last 20 years of the daily rainfall series and removing the days with zero rainfall, the PDF of daily rainfall intervals of 4 mm/day is shown in Figure S1 (supplemental material). There is a general increase in the frequency of daily rainfall events, except for events with daily rainfall less than 4 mm where a reduction is observed. Xavier et al. (1994) had already detected a negative trend in the number of days with rainfall less than 5 mm and a positive trend in the number of days with rainfall in excess of 30 mm for selected months using data from the same station up to 1990. Sugahara et al. (2009) also detected that that high quantiles of daily rainfall in the city of São Paulo have been increasing in magnitude and frequency over time.

The percent difference between the PDF frequencies of the first 20 years and the latter may also be seen in Fig. S1 (supplemental material). The difference reaches 150 % for daily rainfall between 40 and 44 mm and then increases sharply with some oscillation indicating an unstable relationship due to very low frequency of extreme events for the earlier period of 1933–1952.

In view of the change in the shape of the PDF from the earlier part of the record to the last, it is apparent that the frequency of occurrence of extreme daily values has increased. One way to identify long term changes in the precipitation extremes is to determine the daily precipitation value associated to a given frequency of occurrence for successive periods of time. For example, the 95 % percentile of the PDF indicates the daily rainfall value that is not exceeded in 95 % of the cases—or is exceeded in 5 % of the cases.

Figure 4 has been constructed using the daily rainfall value as a reference, hereafter called threshold, defining the 80, 95 and 99 % percentiles. A running window of 20 years starting in 1933 has been used and the PDF determined for each successive 20 years, starting at each successive year. The label indicates the year in the middle of the corresponding 20 year period. The plots include whole year as well as the wet and dry halves of the year (ONDJFM and AMJJAS, respectively) daily rainfall thresholds. Two features stand out upon examination of Fig. 4: an overall increase in the daily rainfall threshold value for the percentiles and a long term modulation of a few decades. For the 80 % threshold it is seen in Fig. 4a that the value increases up to the middle 1950s, shows a gentle decrease up to the early 1980s increasing sharply for about 10 years afterwards and leveling off thereafter. For the drier half of the year, the 95 % threshold (Fig. 4b) shows similar tendencies, except for the last couple of decades when an oscillation of shorter period is detected. In the dry season the threshold decreases in the last two decades. The 99 % threshold (Fig. 4c) has the same general behavior as the 95 % threshold but noisier due to the lower frequency of the most extreme events.

Extreme values are used by various authors in analyzing the changing climate in the past or in future climate projections (e.g. Kharin et al. 2007; Towler et al. 2010; Min et al. 2011). The procedure is based on the fitting of the generalized extreme value (GEV) distribution to the maximum values (Cooley 2009; Zhang et al. 2004). Using the five largest values of daily rainfall, the parameters of the GEV have been obtained here for each successive group of 20 years starting in 1933 and moving the sample by 1 year to obtain the evolution of the extremes. The supplemental material discusses further the GEV analysis and presents more

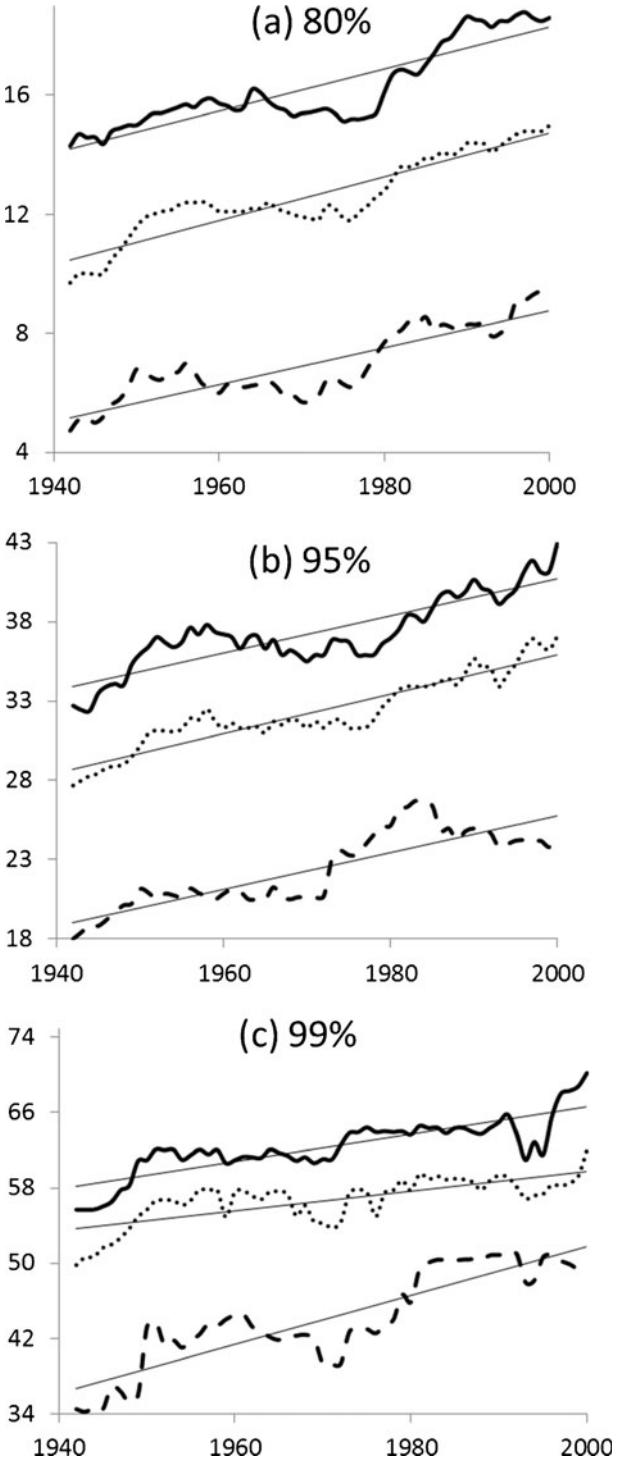

Fig. 4 Evolution of the daily rainfall values defining the percentiles of 80, 95 and 99 % for 20 year intervals for the whole year (*dotted line*), wet season (ONDJFM—*full line*), and dry season (AMJJAS—*dashed line*)

details of its application to the extreme rainfall data. Figure 5 shows the GEV parameters k, σ and μ, respectively the shape parameter, the scale parameter and the location parameter of the distribution, for the wet and dry halves of the year. Of these, the location parameter μ, which indicates the peak in the GEV distribution and thus the most probable value of the extreme daily rainfall, shows a behavior similar to the percentiles, with a long term increase and decadal modulation. The scale parameter σ shows a sharp change in the early 1970s in the wet season, while in the dry season higher values may be found around the 1980s with a decrease in the last 3 decades to values observed in the 1940s. The shape parameter k in the wet season has maximum values between the 1960s and early 1970s while in the dry season the increase of k is after the middle 1980s.

To further quantify the changes in the percentile thresholds, the statistical method discussed in Rodionov (2004) has been employed to detect shifts (i.e., change-points) in the percentile thresholds shown in Fig. 4. The method is based on a sequential data processing technique to test differences in the mean between two data segments of length *L*. Different values of *L* (from 7 to 12 years) were used to test the sensitivity of the method in finding robust change-points. Using L=10 at the 5 % significance level, three change-points in extreme precipitation were detected: early 1950s, mid 1970s and early 1990s. They may be seen as different phases of the multiple decadal oscillation seen in the time series of the percentile thresholds. Change-points in the characteristics of the South American Monsoon System (SAMS) such as the onset, duration and amplitude were also detected in the early 1970s (1971–72) (Carvalho et al. 2010).

A linear fit to the time series of the percentile thresholds and of the location parameter μ has been obtained and is shown in Table S1 (supplemental material) with the associated confidence intervals. The p-value has been computed (e.g. Wilks 2006) to determine the statistical significance at a given test level α. When $p<\alpha$, the correlation is significant at the α-level. All trends have p-values less than 10^{-5}, thus $p << \alpha$ with $\alpha=0.01$ %. The largest detected trend is for the dry season for the 99 % threshold, with 2.5 mm/(day.decade) increase. The 95 % threshold and the location parameter μ show trends close to 1 mm/(day.decade) for both dry and wet seasons. For the wet and dry seasons the trend for the lower percentile thresholds is less than for the higher thresholds indicating that there is a larger increase in frequency for the most extreme cases of daily rainfall. Hourly data has been examined and positive trends in the extreme percentiles for rainfall rate have also been found (not shown).

The behavior of the number of days when rainfall exceeds 40, 60 and 80 mm/day for each season—spring, summer, fall and winter, are shown in Fig. 6. In this case, besides the decadal modulation, it is interesting that for JJA (corresponding to winter period during the dry season) there were no cases of daily precipitation exceeding 60 mm/day up to the middle 1970s. For the 80 mm/day threshold case there was only one case per decade in the first decades. After the early 1970s the number of cases increases, reaching 9 cases in the last decade (2000–2009).

Dry days, defined as those with zero daily rainfall, have also been examined for a 20 years running period and their time evolution for the whole year and for the wet and dry seasons separately and are shown in Figure S1 (supplemental material). Long term modulation with approximate period of 5 decades and no linear trend are observed in this case.

4 Possible causes

To examine possible relationships between the extreme daily precipitation thresholds and climatic indices, the Pearson linear correlation (Wilks 2006) between different pairs has been

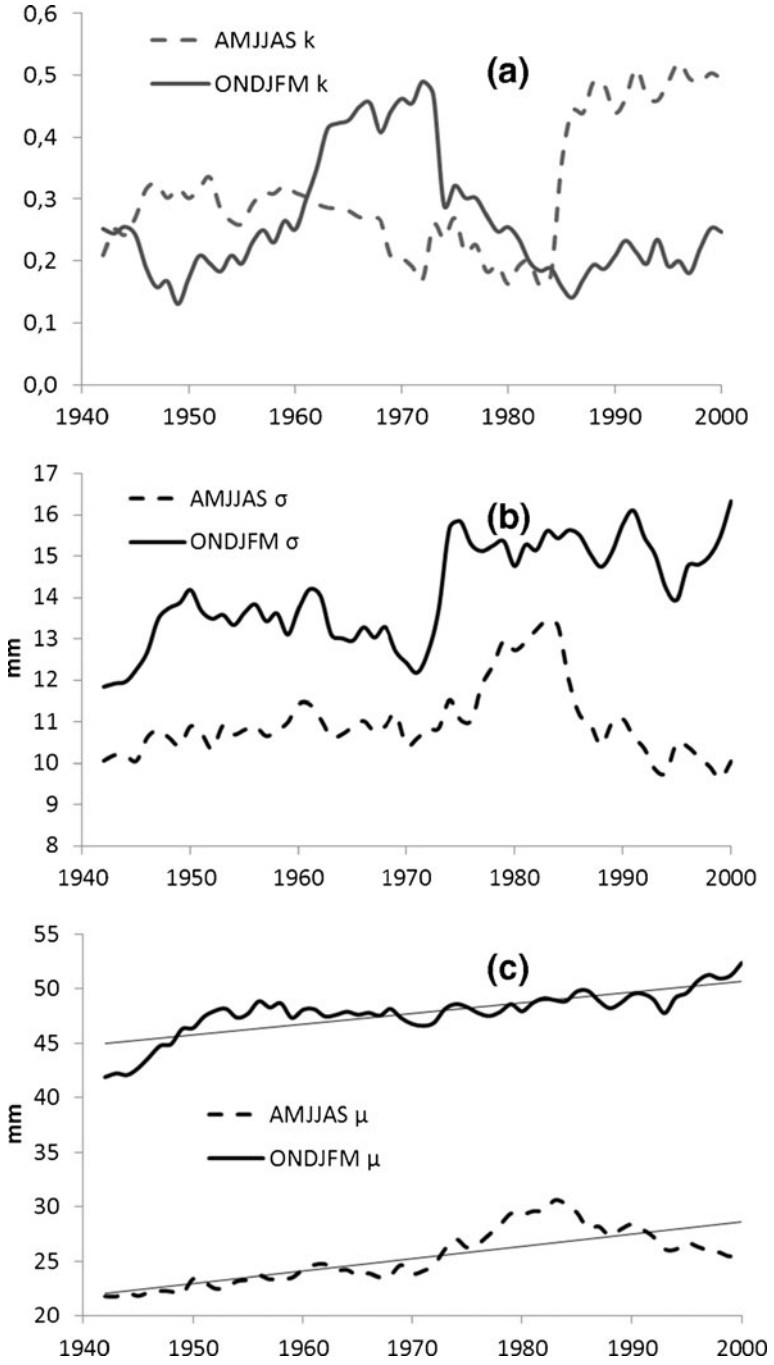

Fig. 5 Evolution of the GEV parameters; **a** shape k; **b** scale σ; location μ. For the wet season (ONDJFM—*full line*) and dry season (AMJJAS *dashed line*)

determined The location parameter μ indicative of the most frequent extreme values is also used in Table 1. Only values significant at the 5 % level are included in Table 1 and the

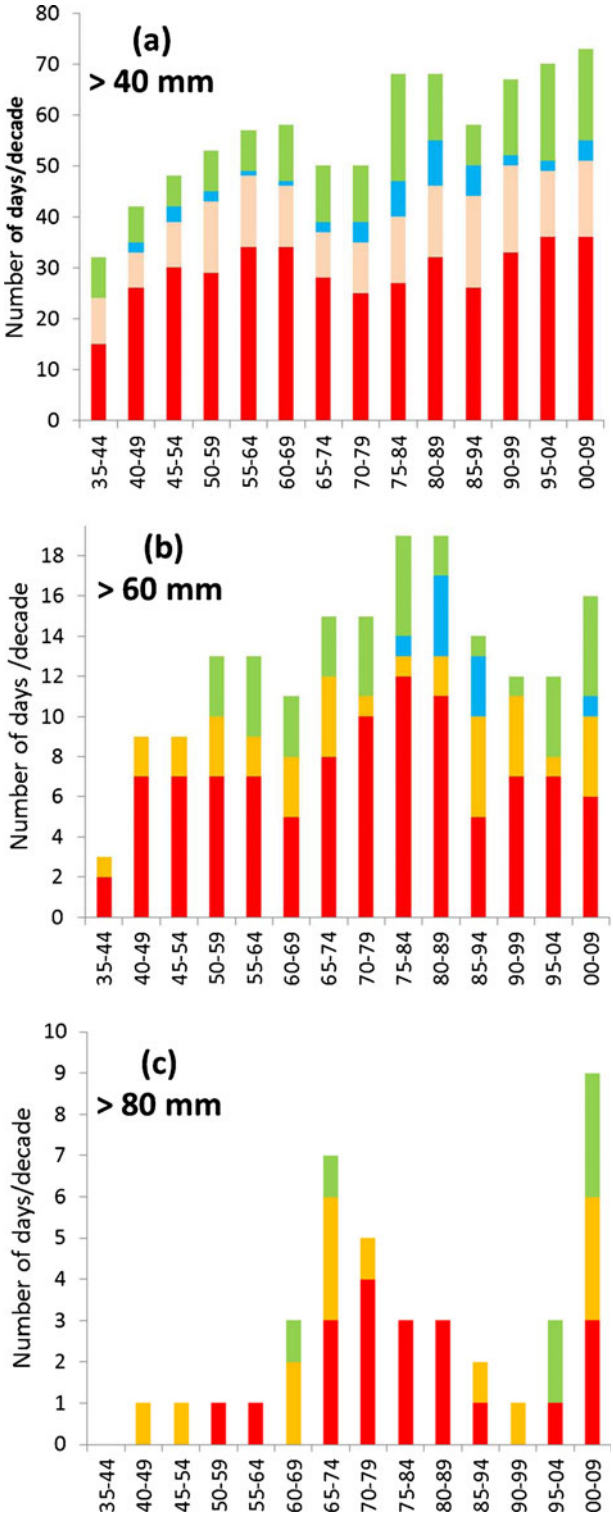

Fig. 6 Evolution of the number of days per decade that the rainfall exceeds **a** 40 mm **b** 60 mm and **c** 80 mm in 10 years for the seasons Spring, September–October–November in *green*, Winter: June–July–August in *blue*, Fall: March–April–May in *orange* and Summer: December–January–February in *red*

Table 1 Pearson correlation coefficient between variables

	PDO	NAO	AMC	ENSO	LISAM	SST	resSST
PDO	1	0.572	-0.301	0.486	0.557	0.456	
NAO	0.572	1	-0.676	0.318	0.454		-0.611
AMC	-0.301	-0.676	1				0.433
ENSO	0.486	0.318		1	0.342		
LISAM	0.557	0.454		0.342	1	0.298	
SST	0.456				0.298	1	0.549
resSST		-0.611	0.433			0.549	1
95% ALL	0.686	0.552		0.362	0.567	0.637	
95% WET	0.568	0.495		0.297	0.557	0.656	
95% DRY	0.855	0.710	-0.436	0.364	0.558		-0.519
99% ALL	0.529	0.369			0.405	0.403	
99% WET	0.429	0.401			0.416	0.462	
99% DRY	0.839	0.663		0.413	0.597	0.489	
μ WET	0.522	0.287			0.498	0.680	
μ DRY	0.823	0.666	-0.479	0.351	0.390		-0.549
σ WET	0.625	0.636	-0.346		0.507		-0.395
σ DRY	0,365						
k WET	-0.543				-0.629		-0.402
k DRY	0.325				0.528	0.565	0.398

Only correlation coefficients with $p<0.05$ are included. Shaded cells have $p<0.01$

shaded cells are significant at the 1 % level. Correlations between climatic indices and between climatic indices and the 95 and 99 % thresholds of the daily precipitation for the whole year and for the wet and dry seasons are shown in Table 1. The correlation between the climatic indices and the GEV parameters k, σ and μ, for the wet and dry seasons are also included. The correlation with SST coastal anomalies (Fig. 1c) are also considered, due to their possible influence in the local circulation, as discussed in the introduction (Freitas et al. 2007, 2009) for the area defined by the square close to the coast in Fig. 1b. A linear fit has been included in Fig. 1c which indicates a 0.11 °C/decade trend. Subtraction of the linear fit from the original SST series yields the residual, hereafter named resSST and also included as an index in Table 1.

The first row of Table 1 shows that the PDO is significantly correlated with all climatic indices except resSST. The PDO column shows the largest correlation coefficients of 0.855 with the 95 % threshold, 0.839 with the 99 % threshold and 0.823 with the location parameter μ in the dry season, significant with $p<0.01$. LISAM and SST also correlate well with all daily rainfall thresholds. For the wet season the highest correlations of the 95, 99 % threshold and of location parameter μ, are with the coastal SST. The scale parameter σ and the shape parameter k do not correlate so well with the climatic indices. Their behavior seems to depend on other causes and will not be investigated further here.

Focusing in the dry and wet season differences and choosing only the cases with p-value significant at the 1 % level, the following variables are listed in decreasing order of the correlation coefficient:

Wet season, 95 %: SST, PDO, LISAM, NAO
Wet Season, 99 %: SST, PDO, LISAM, NAO
Wet season μ: SST, PDO, LISAM
Dry season, 95 %: PDO, NAO, LISAM, ENSO, AMC, resSST
Dry season, 99 %: PDO, NAO, LISAM, SST, ENSO.
Dry season μ: PDO, NAO, LISAM, AMC, resSST

To assure that the correlations found above are representative of the relationship between the two variables, the non-parametric Spearman rank correlation (Table S2—supplemental material) has been calculated (Wilks 2006). The climatic indices with rank correlation significant at the 1 % level with the percentile thresholds and with the GEV location parameter μ are listed below in decreasing order of the Spearman correlation coefficient:

Wet season, 95 %: PDO, SST, LISAM, NAO
Wet season, 99 %: NAO, PDO, LISAM
Wet season μ: PDO, LISAM, SST, NAO
Dry season, 95 %: PDO, NAO, LISAM, AMC, resSST
Dry season, 99 %: PDO, NAO, LISAM, SST, ENSO
Dry season μ: PDO, NAO, LISAM, resSST, AMC

The PDO shows larger correlation than the local SST to the wet season 95 % threshold and for location parameter μ. The SST however does not have significant correlation with the 99 % threshold. For the dry season, the three climatic indices with higher correlations with the percentiles thresholds and for μ are the same from the Spearman and Pearson correlation calculations: PDO, NAO and LISAM.

A straightforward and simple method to quantify the combined role of the climatic indices with respect to the percentile thresholds and to parameter μ is the use of the multiple linear regression fit. Climatic indices are used as predictors and the percentile threshold and μ are the variables to be predicted. The corresponding squared correlation coefficient r^2 is a measure of the variance accounted for by the set of predictors. Table 2 shows the value of r^2 where each successive column represents the explained variance with the addition of each climatic index from the previous column (from left to right). Figure 7 shows the evolution of r^2 with the introduction of each predictor as described in Table 2.

The main result depicted in Fig. 7 is the difference in the dry and wet seasons. The total explained variance after inclusion of the several indices for the dry season for both 95 and 99 % and μ thresholds reaches 85 %. This indicates that most of the increase and variability of the daily precipitation threshold in the dry season is explained by global climatic oscillations represented by the PDO and NAO and of the large scale regional circulation associated with the monsoon index amplitude represented by LISAM, a measure of intensity and length of the wet season of the South American monsoon circulation. The PDO is an index that is associated to large scale SST changes in the Pacific Ocean. The South Pacific Convergence Zone (SPCZ) long term variability is associated to the PDO index. Changes in the position and intensity of the SPCZ have an impact on the structure of the South Atlantic Convergence Zone (SACZ) as shown by Grimm and Silva Dias (1995). The SACZ is associated with the wet season rainfall over most of Southeast Brazil (e.g. Carvalho et al. 2004). The NAO, according to Robertson and Mechoso (1998), is associated to the position and intensity of the subtropical high pressure in the Northern Atlantic, which

Table 2 Variance (r^2) explained by multiple regression with the successive inclusion of climatic indices

r^2	I	II	III	IV	V	VI
95 % WET	SST	SST,PDO	SST, PDO, LISAM	SST, PDO, LISAM, NAO		
	0.431	0.522	0.592	0.671		
99 % WET	SST	SST,PDO	SST, PDO, LISAM	SST, PDO, LISAM, NAO		
	0.213	0.274	0.312	0.369		
95 % DRY	PDO	PDO,NAO	PDO, NAO, LISAM	PDO, NAO, LISAM, resSST	PDO, NAO, LISAM, resSST, AMC	PDO, NAO, LISAM, resSST, AMC, ENSO
	0.732	0.804	0.806	0.846	0.847	0.851
99 % DRY	PDO	PDO, NAO	PDO, NAO, LISAM	PDO, NAO, LISAM, SST	PDO, NAO, LISAM, SST, ENSO	
	0.705	0.755	0.767	0.797	0.850	
μ WET	SST	SST,PDO	SST, PDO, LISAM	SST, PDO, LISAM, NAO		
	0.462	0.512	0.567	0.572		
μ DRY	PDO	PDO,NAO	PDO, NAO, LISAM	PDO, NAO, LISAM, resSST	PDO, NAO, LISAM, resSST, AMC	
	0.677	0.733	0.751	0.825	0.832	

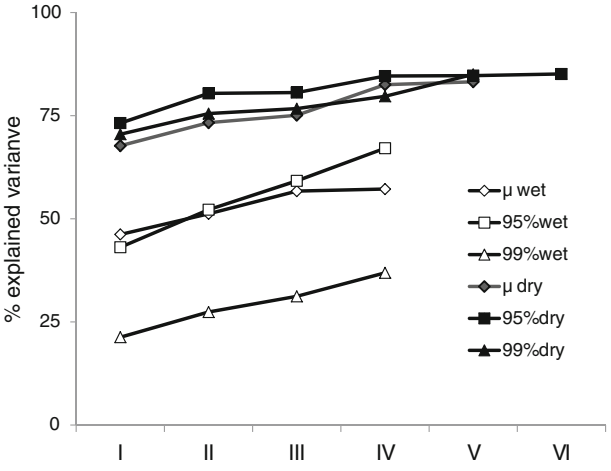

Fig. 7 Percent explained variance by the linear multiple regression for each combination of large scale climatic indices defined in Table 2

affects the low level moisture flux entering the northern portion of the South American continent, ultimately influencing the SACZ precipitation in Southeast Brazil.

In the wet season, the 95 % daily precipitation accumulation threshold is mostly related to the coastal SST and to the PDO, NAO and LISAM and the combined explanation of the variance of the threshold reaches 67 %. For the very extreme cases, corresponding to the 99 % threshold in the wet season, the main conclusion is that the combined indices and local SST explain a much smaller portion of the variance, only 37 %, thus leaving a considerable part of the variance to be explained by other causes.

Considering that the climatic indices include the effects of climate variability and climate change, apart from the increasing temperature of the local SST as well as the large scale circulation associated to the South America Monsoon, the other possible mechanism influencing extreme rainfall in the MASP is the presence of the urban area including the heat island and pollution effects. In the particular case of the MASP, the proximity to the coast and the topography of the plateau (Fig. 1a) need to be considered. As shown in several papers (e.g. Silva Dias et al. 1995; Freitas et al. 2007, 2009) rainfall in the MASP bears a close relationship with the sea breeze coupled with the valley/mountain circulation to the southeast of the city (c.f. Fig. 2a). Freitas et al. (2009) performed several numerical experiments of a severe storm case during the wet season in the MASP. They accounted for the contribution of the local SST anomalies at the coast (approximate location of the box in Fig. 2a) and the presence or absence of the heat island effect in the model simulations. The interaction of the sea breeze with the urban heat island was seen to trigger an enhancement in rainfall in the numerical experiments. Their main conclusion was that the presence of the urban area always contributed to rainfall increase. However, with higher values of local SST they found augmented precipitation in the simulated severe storm, due to higher moisture content brought by the sea breeze. This effect was particularly strong on the eastern side of the city where the sea breeze front first interacts with the urban heat island effect. The location of the IAG station on the southeastern side of the MASP is particularly prone to detect the enhanced rainfall.

From these numerical experiments performed specifically for the MASP and from those performed for other cities (e.g. Carrió et al. 2010) it is plausible to assume that part of the trend and of the variability in daily extreme rainfall may be due to local effects. A more complete investigation of the effect of an evolving urban area through seven decades is under way, following the work of Freitas et al. (2007, 2009).

5 Summary and conclusions

The evolution of extreme daily rainfall in Sao Paulo, Brazil, in the 1933–2010 period has been examined by generating a time series of the frequency of occurrence of daily rainfall thresholds based on the observed PDF for every 20 years starting in successive years. The generalized extreme value distribution parameters have also been obtained using the five larger values of daily rainfall for each year and season as input. The daily rainfall thresholds associated with the 80, 90 and 95 % percentiles of the PDF, and the location parameter μ of the GEV show significant positive linear trends and a multidecadal modulation throughout the period. This is seen for the whole year and for the dry and wet seasons separately. Through a change-point analysis, where changes in averages are tested, a significant change is detected in the early 1970s which is consistent with a change detected in LISAM, the index of the duration of the South American Monsoon system defined by Carvalho et al. (2010).

Climatic indices such as the PDO and NAO play a significant role in explaining the observed trend and variability of the extreme daily rainfall as also does the LISAM index, related to the monsoon circulation in South America. As shown by Carvalho et al. (2010), the LISAM is very well correlated with the intensity and length of the rainy season in central and southeast Brazil. This may explain part of the increase in the frequency of extreme daily precipitation. The SST close to the Atlantic Ocean coast line near the MASP shows a significant linear trend during the same period of the precipitation data (1933–2010) with a multidecadal modulation. The local SST is also related to the trend in the daily rainfall thresholds, especially in the wet season.

More importantly, the climatic indices explain 85 % of the observed variance of the extreme thresholds in the dry season while a smaller portion of this variance is described in the wet season, especially for the most extreme cases of the 99 % percentile of daily precipitation accumulation. This analysis suggests that urban effects can be particularly important to explain the daily rainfall extremes in the wet season. Further investigation is necessary to account for the remaining variance that has been found without explanation based on the large scale climatic indices, especially in the wet season. In order to address this issue, work in progress is focusing on the role of the evolving urban area and the impacts of aerosol from air pollution in cloud microphysics.

Acknowledgments This work has been supported by FAPESP and CNPq. JD acknowledges the support of a NRC Research Associate fellowship. LMVC acknowledges the support of NOAA NA10OAR4310170 and NSF 1126804. PLDSD acknowledges the support of the Inter-American Institute for Global Change Research.

References

Berbery EH, Doyle ME, Barros V (2006) Tendencias regionales en la precipitación. In: Barros V, Clarke R, Silva Días P (eds) El cambio climático en la Cuenca del Plata. CONICET, Buenos Aires, pp 67–92

Bornstein R, Lin Q (2000) Urban heat islands and summertime convective thunderstorms in Atlanta: three case studies. Atmos Environ 34:507–516

Carrió G, Cotton WR (2011) Effects of the urban growth of Houston on convection and precipitation. Part II: dependence of aerosol effects on instability. Atmos Res 97. doi:10.1016/j.atmosres.2011.06.022

Carrió G, Cotton WR, Cheng YY (2010) Effects of the urban growth of Houston on convection and precipitation. Part I: the August 2000 case. Atmos Res 96:560–574. doi:10.1016/j.atmosres.2010.01.005

Carvalho LMV, Jones C, Liebmann B (2004) The South Atlantic Convergence Zone: intensity, form, persistence, and relationships with intraseasonal to interannual activity and extreme rainfall. J Clim 17:88–108. doi:10.1175/1520-0442(2004) 017<0088:TSACZI>2.0.CO;2

Carvalho LMV, Jones C, Silva AE, Liebmann B, Silva Dias PL (2010) The South American Monsoon System and the 1970s climate transition. Int J Climatol 31:1248–1256. doi:10.1002/joc.2147

Chagnon SA (1979) Precipitation changes in summer caused by St. Louis. Science 205:402–404

Changnon SA, Shealy RT, Scott RW (1991) Precipitation changes in fall, winter, and spring caused by St. Louis. J Appl Meteorol 30:126–134

Chen WY, van den Dool H (2003) Sensitivity of teleconnection patterns to the sign of their primary action center. Mon Wea Rev 131:2885–2899

Chiang JCH, Vimont DJ (2004) Analogous meridional modes of atmosphere–ocean variability in the tropical Pacific and tropical Atlantic. J Clim 17(21):4143–4158

Cooley D (2009) Extreme value analysis and the study of climate change. Climatic Change 97:77–83. doi:10.1007/s10584-009-9627-x

Dufek AS, Ambrizzi T (2008) Precipitation variability in São Paulo State, Brazil. Theor Appl Climatol 93:167–178. doi:10.1007/s00704-007-0348-7

Freitas ED, Rozoff CM, Cotton WR, Silva Dias PL (2007) Interactions of an urban heat island and sea breeze circulations during winter over the Metropolitan Area of São Paulo—Brazil. Boundary - Layer Meteorol 122:43–65

Freitas ED, Silva Dias PL, Carvalho VSB, Rocha CRM, Martins LD, Martins JA, Andrade MF (2009) Factors involved in the formation and development of severe weather conditions over the megacity of São Paulo. Eighth Symposium on the Urban Environment, Modeling and Forecasting in Urban Areas. Proceedings of the 89th AMS Annual Meeting, 2009

Grimm AM, Silva Dias PL (1995) Analysis of tropical–extratropical interactions with influence functions of a barotropic model. J Atmos Sci 52:3538–3555

Haylock MR, Peterson TC, Alves LM, Ambrizzi T, Anunciação YMT, Baez J, Barros VR, Berlato MA, Bidegain M, Coronel G, Corradi V, Garcia VJ, Grimm AM, Karoly D, Marengo JA, Marino MB, Moncunill DF, Nechet D, Quintana J, Rebello E, Rusticucci M, Santos JL, Trebejo I, Vincent LA (2006) Trends in total and extreme South American Rainfall in 1960–2000 and links with Sea Surface Temperature. J Clim 19:1490–1512

Hurrell JW (1995) Decadal trends in the North Atlantic Oscillation and relationships to regional temperature and precipitation. Science 269:676–679

Janowiak JE, Gruber A, Kondragunta CR, Livezey RE, Huffman GJ (1998) A comparison of the NCEP–NCAR reanalysis precipitation and the GPCP rain gauge–satellite combined dataset with observational error considerations. J Clim 11:2960–2979. doi:10.1175/1520-0442(1998) 011<2960:ACOTNN>2.0.CO;2

Kalnay E, Cai M (2003) Impact of urbanization and land-use change on climate. Nature 423:528–531

Kalnay E et al (1996) The NCEP/NCAR reanalysis 40-year project. Bull Am Meteorol Soc 77:437–471

Kharin VV, Zwiers FW, Zhang X, Hegerl GC (2007) Changes in temperature and precipitation extremes in the IPCC ensemble of global coupled model simulations. J Clim 20:1419–1444. doi:10.1175/JCLI4066.1

Liebmann B, Jones C, Carvalho LMV (2001) Interannual variability of daily extreme precipitation events in the state of São Paulo, Brazil. J Clim 14:208–217

Mantua NJ, Hare SR, Zhang Y, Wallace JM, Francis RC (1997) A Pacific interdecadal climate oscillation with impacts on salmon production. Bull Am Meteorol Soc 78:1069–1079

Marengo JA, Liebmann B, Kousky VE, Filizola NP, Wainer IC (2001) Onset and end of the rainy season in the Brazilian Amazon basin. J Clim 14:833–852. doi:10.1175/1520-0442(2001) 014<0833:OAEOTR>2.0.CO;2

Min S-K, Zhang X, Zwiers FW, Heger GC (2011) Human contribution to more-intense precipitation extremes. Nature 470:378–381. doi:10.1038/nature09763

Penalba O, Robledo FA (2010) Spatial and temporal variability of the frequency of extreme daily rainfall regime in the La Plata Basin during the 20th century. Clim Chang 98(3–4):531–550

Pereira Filho AJ, Santos PM, Camargo R, Festa M, Funari FL, Salum ST, Oliveira CT, Santos EM, Lourenço PR, Silva EG, Garcia W, Fialho MA (2007) Caracterização do Clima e sua Evolução na Região Metropolitana de São Paulo. In: Pereira Filho; Marques dos Santos; Xavier. (Org.) Evolução do Tempo e do Clima na Região Metropolitana de São Paulo, 1 ed. Linear B, São Paulo, vol 1, pp 99–120 (in Portuguese)

Rana A, Uvo CB, Bengtsson L, Parth Sarthi P (2011) Trend analysis for rainfall in Delhi and Mumbai, India. Clim Dyn. doi:10.1007/s00382-011-1083-4

Robertson AW, Mechoso CR (1998) Interannual and decadal cycles in river flows of southeastern South-America. J Clim 11:2570–2581

Rodionov SN (2004) A sequential algorithm for testing climate regime shifts. Geophys Res Lett 31:L09204. doi:09210.01029/02004GL019448,012004

Satyamurty P, Nobre CA, Silva Dias P (1998) South America. In: Karoly D, Vincent DG (ed) Meteorology of the southern hemisphere. Meteorol Monogr 27, 119–139

Shepherd JM, Pierce H, Negri AJ (2002) Rainfall modification by major urban areas: observations from spaceborne rain radar on the TRMM satellite. J Appl Meteorol 41:689–701

Silva Dias MAF, Vidale PL, Blanco CMR (1995) Case study and numerical simulation of the summer regional circulation in Sao Paulo, Brazil. Boundary - Layer Meteorol 74:371–388

Silva AE, Carvalho LMV (2007) Large-scale index for South America Monsoon (LISAM). Atmos Sci Lett 8:51–57. doi:10.1002/asl.150

Sugahara S, Rocha RP, Silveira R (2009) Non-stationary frequency analysis of extreme daily rainfall in Sao Paulo, Brazil. Int J Climatol 29:1339–1349. doi:10.1002/joc.1760

Sugahara S, Rocha RP, Ynoue RY, Silveira RB (2011) Homogeneity assessment of a station climate series (1933–2005) in the Metropolitan Area of São Paulo: instruments change and urbanization effects. Theor Appl Climatol. doi:10.1007/s00704-011-0485-x

Towler E, Rajagopalan B, Gilleland E, Summers RS, Yates D, Katz RW (2010) Modeling hydrologic and water quality extremes in a changing climate: a statistical approach based on extreme value theory. Water Resour Res 46:W11504. doi:10.1029/2009WR008876

Villaça FJM (1978) The territorial structure of the Brazilian Southern megacity (A estrutura territorial da metrópole sul brasileira). Ph. D. Thesis. FFLCH/USP, Departamento de Geografia. (in Portuguese)
Wilks DS (2006) Statistical methods in the atmospheric sciences, 2nd edn. International Geophysics Series, vol 91, Academic Press, 627 pp
Wolter K, Timlin MS (1993) Monitoring ENSO in COADS with a seasonally adjusted principal component index. Proc. of the 17th Climate Diagnostics Workshop, Norman, OK, NOAA/NMC/CAC, NSSL, Oklahoma Clim. Survey, CIMMS and the School of Meteor., Univ. of Oklahoma, 52–57
Xavier TMS, Xavier AFS, Silva Dias MAF (1994) Evolução da precipitação diária num ambiente urbano: o caso da cidade de São Paulo. Rev Bras Meteorol 9:44–53 (in Portuguese)
Zhang Y, Wallace JM, Battisti DS (1997) ENSO-like interdecadal variability: 1900–93. J Clim 10:1004–1020
Zhang X, Zwiers FW, Li G (2004) Monte Carlo experiments on the detection of trends in extreme values. J. Clim 17:1945–1952